EXPERIMENTAL EVALUATION OF A MINIATURE ROTARY COMPRESSOR FOR APPLICATION IN ELECTRONICS COOLING

Abhijit A Sathe, Eckhard A Groll* and Suresh V Garimella
Cooling Technologies Research Center, School of Mechanical Engineering
Purdue University, West Lafayette, Indiana 47907, USA

* Corresponding author, email: groll@purdue.edu

ABSTRACT

This paper describes performance measurements on a prototype miniature rotary compressor with refrigerant R134a using a compressor load stand based on a hot-gas bypass design. The hermetically sealed rolling piston compressor runs on a 24 V DC power supply. Because of its small size and compact form factor, it can potentially be used in a miniature vapor compression refrigeration system for electronics cooling applications.

Compressor tests are conducted for varying suction pressures, pressure ratios, and rotational speeds. For each test, the refrigerant mass flow rate, electrical power consumption, and the suction and discharge temperature and pressure are recorded, at a suction superheat of 5 K. Using the experimental data, the compressor volumetric and overall isentropic efficiencies are calculated. Also, by assuming a subcooling of 5 K in the condenser, a hypothetical cooling capacity of the system and the corresponding COP are calculated. The volumetric efficiency ranges from 73% to 90% and the overall isentropic efficiency varies from 44% to 70% for pressure ratios between 2 and 3.5. For this range of pressure ratios, the estimated cooling capacity and the COP vary from 163 W to 489 W and 2.1 to 7.4, respectively.

1. INTRODUCTION

It has been predicted that the heat dissipation from a single electronic chip package will rise to 200 W in 2008 for high-performance systems (International Technology Roadmap for Semiconductors, 2006). It is also anticipated that traditional electronics cooling approaches such as forced convective air cooling using conventional heat sinks will soon reach their limits for meeting the dissipation needs of emerging high-performance electronics systems (Krishnan et al., 2007). Several alternative cooling approaches have been studied in the literature to achieve the required heat dissipation rates, while satisfying the required reliability, size and cost considerations. These approaches include heat pipes, liquid immersion, jet impingement and sprays, microchannel heat sinks, thermoelectric cooling, and refrigeration (Garimella, 2006). Vapor compression refrigeration appears to be among the more promising techniques because of its ability to operate at varying loads and high ambient temperatures. It is also one of the very few cooling methods in which the source temperature can be lower than the sink temperature. Trutassanawin et al. (2006) experimentally investigated a miniature refrigeration system using two commercially available refrigerant compressors and concluded that for developing an efficient and reliable miniature refrigeration system, a miniature refrigerant compressor is required that can satisfy the necessary pressure rise and pumping needs, while at the same time being compact in size and form factor. Sathe et al. (2004) investigated a novel electrostatically actuated diaphragm compressor for use in miniature-scale compression technology, but highlighted the manufacturing challenges involved in fabricating such a device. As another alternative a miniature rolling-piston rotary compressor designed and fabricated by Aspen Compressor, LLC, is investigated in this study.

2. EXPERIMENTAL SETUP

The miniature rotary compressor operates with a rolling piston mechanism. It uses a brushless electric motor that runs on 24 V DC power supply. Figure 1 shows the important external dimensions of the compressor, while its specifications are given in Table 1.

For testing the miniature rotary compressor, a hot gas bypass load stand was designed. A detailed schematic diagram of the hot gas bypass load stand and the corresponding pressure-enthalpy diagram are shown in Figure 2.

The main idea behind this concept is to use an intermediate pressure as a pressure anchor for the test stand by condensing a fraction of the refrigerant flow. Using this stable anchoring pressure, the suction and discharge pressures are controlled by using appropriate metering valves in the discharge line and bypass line. The superheat at the compressor inlet is controlled by metering a small amount of condensed liquid refrigerant flow into the bypass flow. Low-pressure, slightly superheated refrigerant vapor enters the compressor (state point 1). The compressor discharges high-pressure, high-temperature refrigerant at state point 2, which is throttled to the intermediate pressure at state point 3. At this point, any oil in the discharge flow is separated from the refrigerant using an oil separator. This is done to reduce the oil concentration in the refrigerant flow before passing it through the mass flow meter in the vapor line so that only the refrigerant mass flow rate is measured. After passing through the mass flow meter, the refrigerant flow is split. Most of the refrigerant flow enters the bypass loop where it is throttled to the suction pressure (state point 4) using an expansion valve. The remaining flow passes through a condenser where it is condensed to a saturated liquid state (state point 5), throttled to the suction pressure and mixed with the bypassed flow such that the compressor suction state is restored.

Testing with the hot-gas bypass loop offers the following advantages over a full compressor calorimeter:
1. A hot-gas bypass compressor test stand is easier to construct and operate than a full compressor calorimeter since it consists of fewer components.
2. The operating conditions of discharge pressure, suction pressure, and suction superheat are directly controlled by three expansion valves (discharge line, bypass line, and primary line). This control method allows for faster transition from one set of operating conditions to the next and also a more stable operating condition compared to a full compressor calorimeter.
3. During normal operation of the loop, approximately two-thirds of the refrigerant flow passes through the bypass line. Hence the required condenser cooling capacity is quite low. This allows the use of a small-capacity condenser.

3. MEASUREMENTS AND DATA REDUCTION

Experimental tests on the compressor are conducted at three different suction pressures, four pressure ratios, and three compressor rotational speeds, according to the test matrix in Table 2. The following parameters are directly measured using the instrumentation: 1) Suction pressure and temperature, 2) discharge pressure and temperature, 3) refrigerant mass flow rate, 4) electrical power consumed by the compressor (by measuring DC voltage and current supplied to the main circuit board), and 5) compressor rotational speed (by measuring the DC voltage supplied to the secondary circuit board). The uncertainties of the measured and calculated parameters (Moffat, 1988) are given in Table 3.

The measured refrigerant mass flow rate and compressor power consumption are corrected using the superheat correction (Dabiri and Rice, 1982) such that the compressor suction superheat is 5 K for all of 36 data points.

$$\frac{\dot{m}}{\dot{m}_{measured}} = 1 + F\left(\frac{\rho_{new}}{\rho_{measured}} - 1\right)$$

$$\frac{\dot{W}}{\dot{W}_{measured}} = \frac{\dot{m}_{new}}{\dot{m}_{measured}} \frac{(h_{2s} - h_1)_{new}}{(h_{2s} - h_1)_{measured}}$$

(1)

where F is the correction factor ($F = 0.75$).

The following performance parameters are calculated:
1. Volumetric efficiency

$$\eta_{volumetric} = \frac{\dot{m} \cdot v_{suction}}{RPM \cdot Vol}$$

(2)

The suction specific volume is calculated as a function of suction temperature and pressure. The compressor displacement volume is obtained from the manufacturer's specifications.

2. Overall isentropic efficiency

$$\eta_{isen,overall} = \frac{\dot{m} \cdot (h_{discharge,isen} - h_{suction})}{\dot{W}}$$ (3)

The suction enthalpy is calculated as a function of the suction temperature and pressure. The isentropic discharge enthalpy is calculated by assuming constant entropy for the compression process. Hence,

$$h_{discharge,isen} = f(s_{suction}, P_{discharge})$$ (4)

where the suction entropy is calculated as a function of the suction temperature and pressure.

3. Cooling capacity

$$\dot{Q} = \dot{m} \cdot (h_{suction} - h_{evaporator,in})$$ (5)

The cooling capacity is calculated by assuming that the compressor is a part of a hypothetical vapor compression refrigeration system. The following assumptions are made:
- The pressure drops in the condenser and the evaporator of the hypothetical system are neglected.
- A subcooling of 5 K is assumed at the condenser outlet.
- An isenthalpic pressure drop is assumed in the throttle device.

The evaporator inlet enthalpy is calculated as a function of the condenser outlet enthalpy and the suction pressure. The condenser discharge enthalpy is calculated as a function of the compressor discharge pressure and the condenser subcooling.

4. Coefficient of performance (*COP*)

$$COP = \frac{\dot{Q}}{\dot{W}}$$ (6)

5. RESULTS

The compressor performance parameters defined in the previous section are plotted as a function of the compressor pressure ratio for the different suction pressures and compressor rotational speeds. Figure 3 shows the variation of volumetric efficiency with pressure ratio. In most of the cases (the one outlier in the tests seems to be the data point at a pressure ratio of 3.5 and suction pressure of 3 bar), the volumetric efficiency decreases slightly with increase in the pressure ratio and ranges from 90% to 73%. The performance measurements indicate that the volumetric efficiency does not change with speed for otherwise similar operating conditions. Figure 4 presents the variation of the overall isentropic efficiency of the compressor as a function of the pressure ratio. Although a clear trend is not observed, it can be seen that the compressor speed does not have much influence on the overall isentropic efficiency. The overall isentropic efficiency varies in the range of 44% to 70%. It must be noted here that this efficiency includes the power loss at the compressor electronic circuit board.

The theoretical cooling capacity of the system is plotted as a function of the pressure ratio in Figure 5. The cooling capacity decreases with an increase in pressure ratio (the evaporator inlet enthalpy in equation (5) decreases with increase in the compressor discharge pressure, which reduces the enthalpy difference available in the evaporator resulting in a drop in the observed drop in cooling capacity). In addition, the compressor speed has a significant influence on the cooling capacity. An increase in the compressor speed leads to higher refrigerant mass flow rates. Hence, the cooling capacity increases linearly with speed. The highest cooling capacity of 490 W is observed at a speed of 6000 rpm. It may be noted that the maximum continuous compressor speed is nominally 6,500 rpm. In terms of noise level and performance, it seems that the compressor runs best at approximately 4,000 rpm.

Finally, the system coefficient of performance (COP) is shown in Figure 6 as a function of pressure ratio. The COP decreases rapidly as the pressure ratio increases. Here too, the performance measurements indicate that the COP

does not change with speed for otherwise similar operating conditions. For the given set of tests, the COP varied from 2.1 to 7.4.

As mentioned above, Trutassanawin et al. (2006) developed and tested a bread board miniature refrigeration system for electronics cooling using microchannel heat exchangers and commercially available compressors. Two different compressors were used: 1) a rotary compressor manufactured by Engel, and 2) a reciprocating compressor manufactured by Hitachi. Table 4 provides a comparison of these two compressors and also the rotary compressor investigated here in terms of geometric features and performance. It clearly demonstrates that the sizing of the compressor holds the key to an efficient miniature refrigeration system for electronics cooling. The two compressors tested by Trutassanawin et al. (2006) were oversized for the electronics cooling application and offered relatively poor performance. The Aspen rotary compressor, however, has a much smaller displacement volume and provides good system performance.

6. CONCLUSIONS

A miniature rolling-piston rotary compressor prototype is experimentally tested using a hot-gas bypass circuit design and the refrigerant R134a. The tests were conducted for different suction pressures, pressure ratios and rotational speeds. Important performance parameters were either directly measured or calculated using basic thermodynamic relations. The experimental results indicate that the compressor renders good volumetric and overall isentropic efficiencies.

The compressor performance has been compared to that of two different compressors tested in the literature as part of a miniature refrigeration system for electronics cooling. The comparison indicates that the compressor investigated here performs better in terms of the efficiencies and cycle COP. With its small size and low weight, the compressor investigated here has the potential for use in miniature vapor compressor refrigeration systems for electronics cooling, such as for desktop computer applications.

ACKNOWLEDGEMENT

NOMENCLATURE

Symbols: Subscripts:

η	Efficiency [%]	*isen* Isentropic
ρ	Density [kg/m^3]	
F	Superheat correction factor [-]	
h	Enthalpy [J/kg]	
$\dot{m}$	Refrigerant mass flow rate [kg/s]	
$\dot{W}$	Electrical power [W]	
P	Pressure [bar]	
Vol	Compressor displacement [m^3]	
v	Specific volume [m^3/kg]	
s	Entropy [J/kg-K]	
$\dot{Q}$	Cooling capacity [W]	
RPM	Rotational speed [rpm]	

REFERENCES

1. Garimella, S. V., 2006, "Advances in mesoscale thermal management technologies for microelectronics", Microelectronics Journal, Vol. 37, No. 11, Nov. 2006, pp. 1165-1185.
2. Dabiri, A. E., and Rice, C. K., 1981, "A Compressor Simulation Model with Corrections for the Level of Suction Gas Superheat," ASHRAE Transactions, Vol. 87, Part 2, pp.771-782.
3. International Technology Roadmap for Semiconductors, 2006 edition, "Assembly and packaging", Semiconductor Industry Association.
4. Krishnan, S., Garimella, S. V., Chrysler, G. M., Mahajan, R. V., 2007, "Towards a thermal Moore's law", IEEE Transactions on Advanced Packaging, Vol. 30, No. 3, 2007, pp. 462-474.
5. Moffat, R. J, 1988, "Describing the Uncertainties in Experimental Results," Experimental Thermal and Fluid Science, Vol. 1, pp. 3-17.
6. Sathe, A. A., Cremaschi, L., Groll, E. A., Garimella, S. V., 2006, "A New Model for an Electrostatically Actuated Miniature-Scale Diaphragm Compressor for Electronics Cooling", 18th International Compressor Engineering Conference at Purdue University, Jul 14-16, 2006.
7. Trutassanawin, S., Groll, E. A., Garimella, S. V. and Cremaschi, L., 2006, "Experimental investigation of a miniature-scale refrigeration system for electronics cooling," IEEE Transaction on Components and Packaging Technologies, Vol. 29, No. 3, pp. 678-687.

Table 1. Specifications of the rotary compressor tested.

Refrigerant	R134a
Lubrication oil	Nu Calgon RL68H Polyol ester oil
Compressor type	Rotary (rolling piston)
Compressor displacement	1.4 cc
Compressor speed	Variable
Speed range	2000 – 6500 RPM
Motor	Brushless DC
Voltage	24 V DC
Maximum current	12 Amps continuous
Evaporator temperature range	-18 – 24 °C
Condenser temperature range	27 – 71 °C
Maximum discharge temperature	130 °C
Maximum compression ratio	8:1

Table 2. Rotary compressor test matrix.

Test No	Speed (RPM)	Suct. Pr. (bar)	Dis. Pr. (bar)	Test No	Speed (RPM)	Suct. Pr. (bar)	Dis. Pr. (bar)	Test No	Speed (RPM)	Suct. Pr. (bar)	Dis pr. (bar)
A1		3	6	A13		3	6	A25		3	6
A2			7.5	A14			7.5	A26			7.5
A3			9	A15			9	A27			9
A4			10.5	A16			10.5	A28			10.5
A5	3000	4	8	A17	4500	4	8	A29	6000	4	8
A6			10	A18			10	A30			10
A7			12	A19			12	A31			12
A8			14	A20			14	A32			14
A9		5	10	A21		5	10	A33		5	10
A10			12.5	A22			12.5	A34			12.5
A11			15	A23			15	A35			15
A12			17.5	A24			17.5	A36			17.5

Table 3. Uncertainties in the measurements and calculated values.

Measured value	Uncertainty		Calculated value	Uncertainty
Pressures	± 1 %		Volumetric efficiency	± 3.0 %
Temperatures	± 1 °C		Overall isentropic efficiency	± 8.6 %
Mass flow rate	± 0.1 %		Cooling capacity	± 3.1 %
Electrical power	± 4 %		COP	± 8.6 %
RPM	± 1 %			

Table 4. Comparison of miniature refrigerant compressors.

	Engel rotary compressor*	Hitachi reciprocating compressor*	Aspen rotary compressor
Dimensions			
Height (mm)	166	195	78
Length/diameter (mm)	Φ 85	204	Φ 56
Width (mm)	-	13 mm	-
Displacement (cc)	2.3	2.0	1.4
Weight (kg)	2.8	4.3	0.6
Performance with refrigerant R134a			
Pressure ratio	2.1 – 3.2	1.9 – 3.0	2.0 – 3.5
Speed (rpm)	2000	2000	3000 – 6000
Volumetric efficiency (%)	57.0 – 79.3	58.1 – 73.0	73.2 – 90.5
Overall isentropic efficiency (%)	40.6 – 59.5	43.2 – 56.5	44.1 – 70.3
Cooling capacity (W)	130.1 – 256.4[†]	152.2 – 208.8[†]	160.2 – 489.6[ζ]
System COP	3.0 – 5.7	2.6 – 3.7	2.1 – 7.4

* – Experimental data from Trutassanawin et al. (2006)

[†] – Measured cooling capacity

[ζ] – Calculated cooling capacity

Note: All dimensions are in inches

(a)   (b)
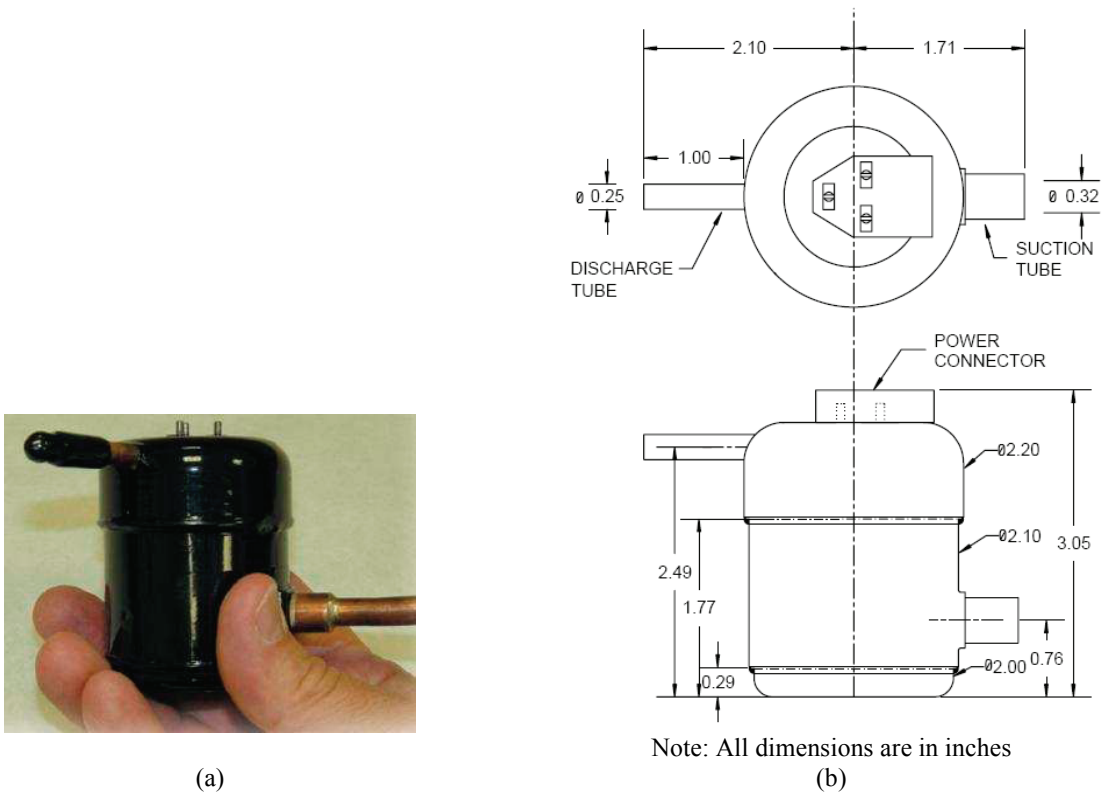
Figure 1. (a) The Aspen Compressor prototype, and (b) external dimensions of the compressor (Courtesy of Aspen Compressor, LLC.).
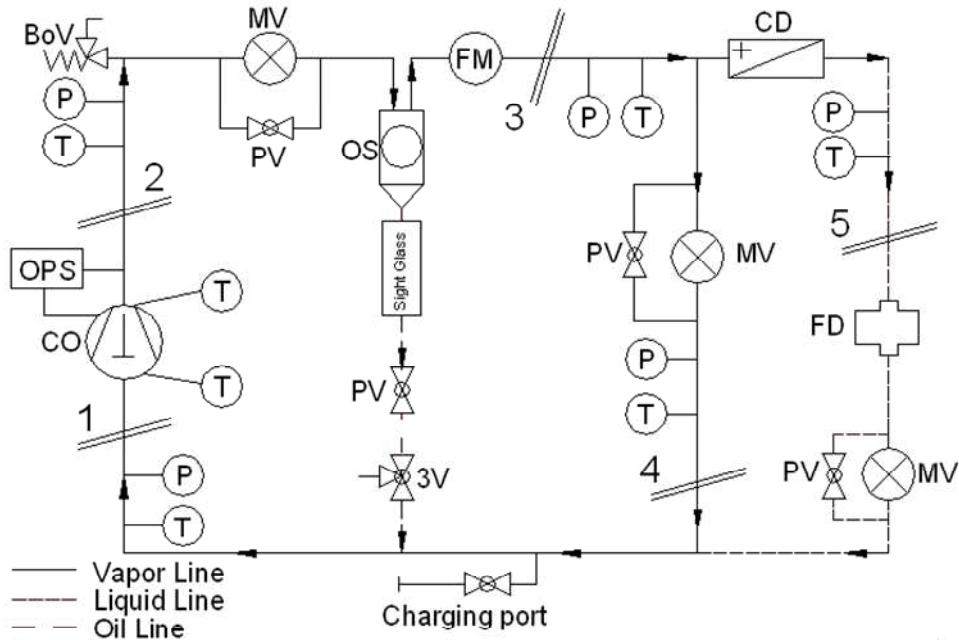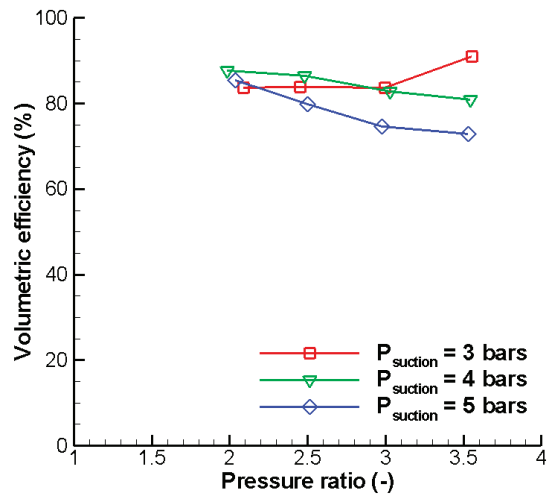
(a)
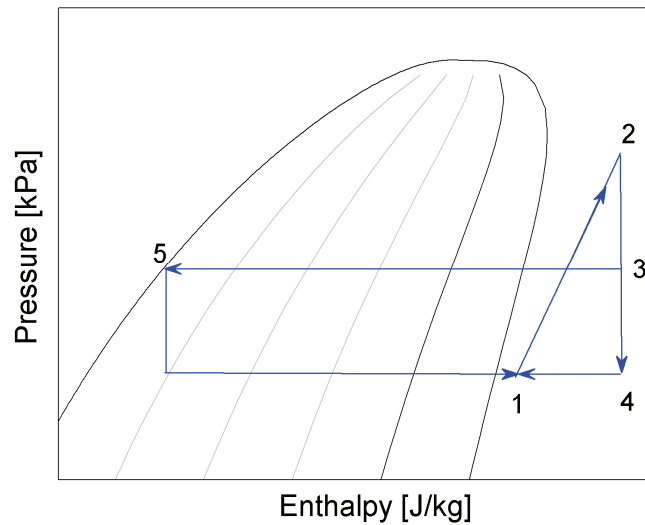
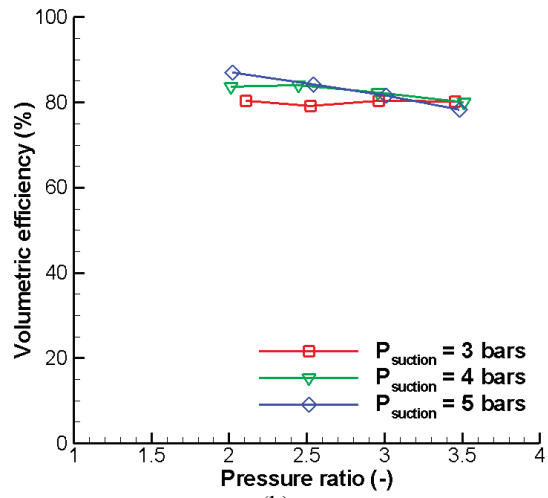
(b)

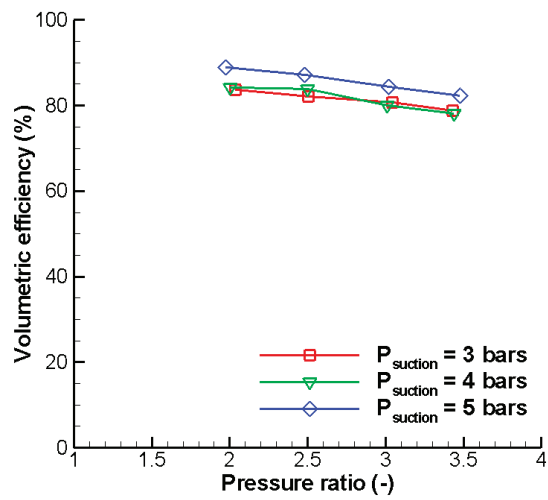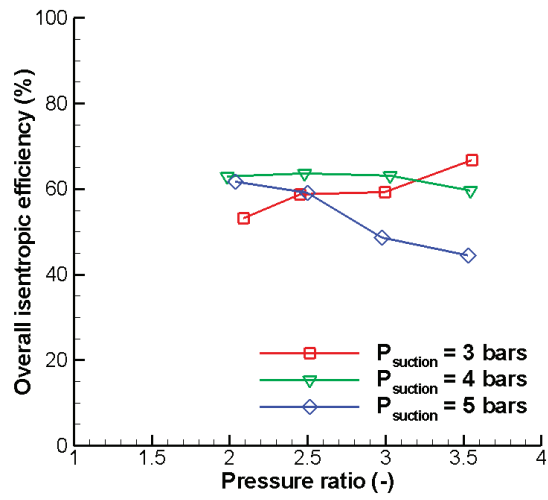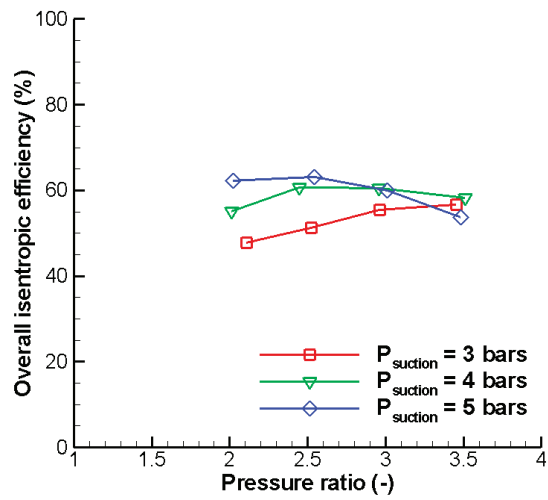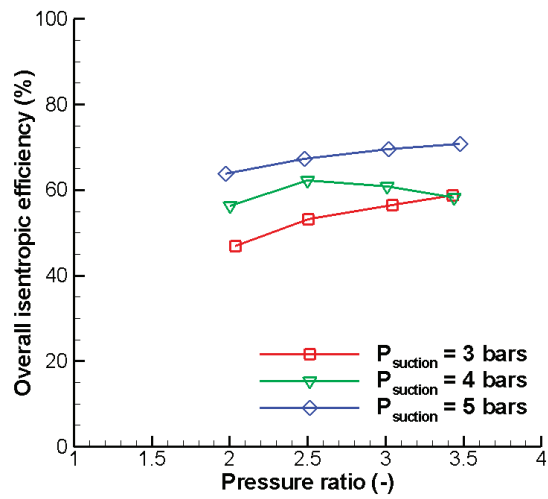Figure 2. The hot gas bypass loop for compressor testing: (a) schematic diagram, and (b) on a P-h diagram.

Figure 3. Variation of compressor volumetric efficiency with pressure ratio for rotational speeds of (a) 3000 rpm, (b) 4500 rpm, and (c) 6000 rpm.
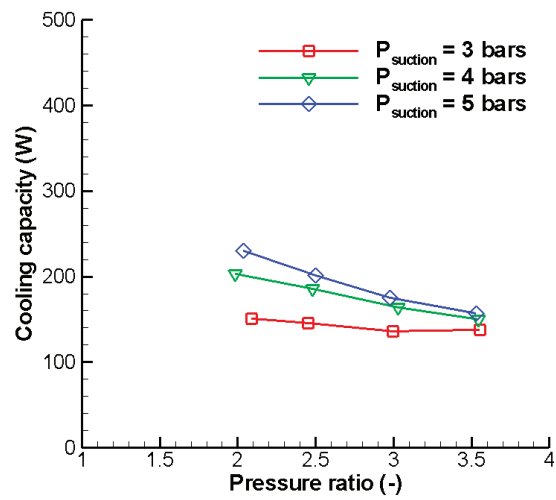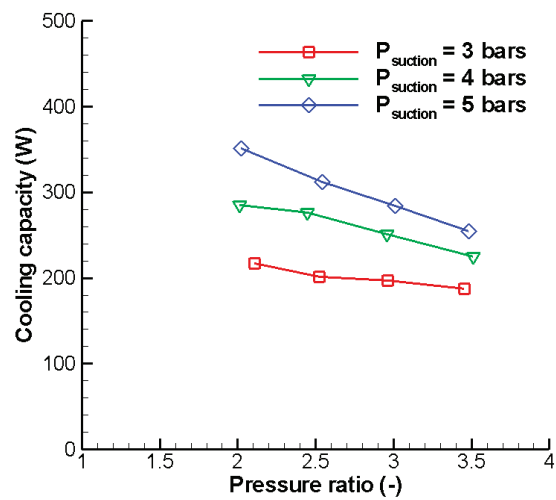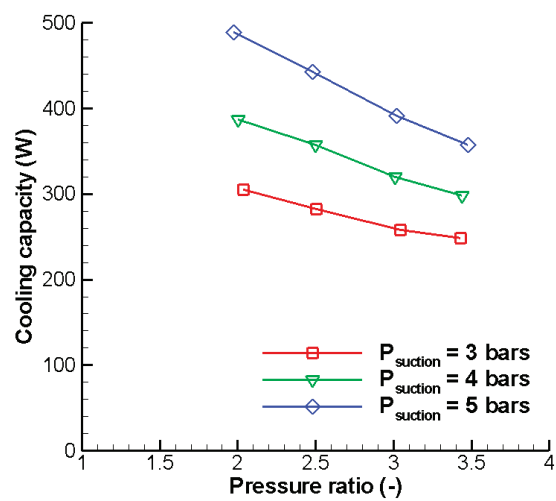
Figure 4. Variation of compressor overall isentropic efficiency with pressure ratio for rotational speeds of (a) 3000 rpm, (b) 4500 rpm, and (c) 6000 rpm.
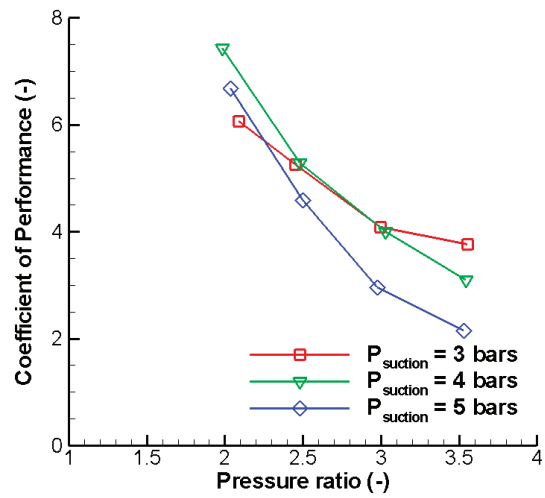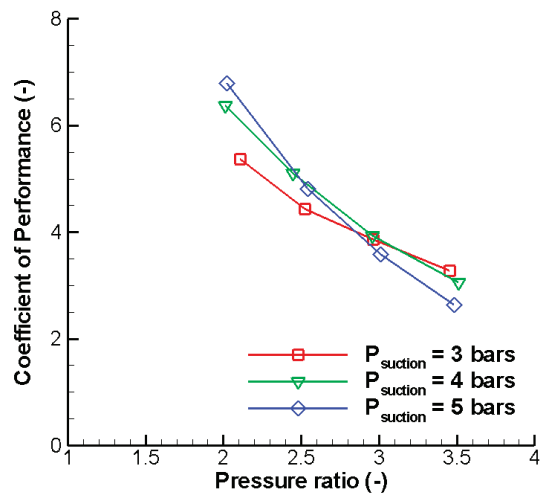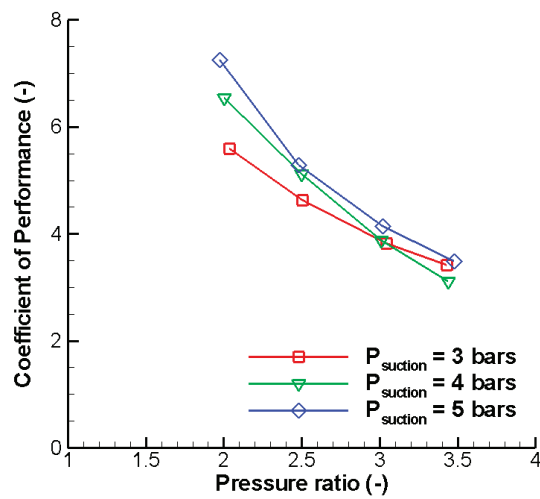
Figure 5. Variation of compressor cooling capacity with pressure ratio for rotational speeds of (a) 3000 rpm, (b) 4500 rpm, and (c) 6000 rpm.

Figure 6. Variation of system COP with pressure ratio for rotational speeds of (a) 3000 rpm, (b) 4500 rpm, and (c) 6000 rpm.